Alloying of Zn-Al-Mg coatings for corrosion stability improvement

T. Prosek[1], F. Goodwin[2], D. Thierry[1]

[1] Institut de la Corrosion / French Corrosion Institute
220 rue Pierre Rivoalon, 29200 Brest, France
Phone: +33 630 614 808
Email: tomas.prosek@institut-corrosion.fr

[2] International Zinc Association
1822 East NC Hwy 54, Suite 120, Durham, NC 27713, USA
Phone: +1 919 361 4647
Email: fgoodwin@zinc.org

ABSTRACT

Aluminum and magnesium are known for their ability to improve corrosion performance of zinc coatings used for steel protection in automotive applications. To investigate inhibiting properties of other elements, series of model Zn-X, Zn-Al-X, Zn-Mg-X and Zn-Al-Mg-X alloys containing 0.2–2 wt.% of titanium, mischmetal (mixture of cerium and other lanthanides), zirconium, molybdenum, chromium, boron, gallium, indium, copper, nickel, calcium, manganese and silicon were prepared and characterized in terms of chemical and phase composition. Corrosion performance of the alloys was assessed by measuring mass loss after a cyclic accelerated test used in the automotive industry (ECC1). A set of promising materials was exposed at a marine exposure site with high corrosivity. Most experiments were carried out with openly exposed samples but crevice samples simulating hem flanges were used as well. Electrochemical measurements were performed to verify if the materials were able to provide galvanic protection to steel in defects.

On open surfaces, Mg and Al showed the strongest corrosion inhibiting effect. When exposed to marine climate, it was beneficial to combine both elements. The corrosion stability of Zn-Al-Mg was further improved by addition of a fourth element. Quaternary Zn-Al-Mg-X alloys outperformed binary Zn-X and ternary Zn-Al-X and Zn-Mg-X alloys.

Higher corrosion rates compared to open configurations were observed in confined zones due to separation of anodic and cathodic sites. Strong inhibition with Mg and detrimental effect of Al on corrosion in confined zones was found. It is expected that the detrimental effect of Al was more due to coarser microstructures leading to formation of micro-galvanic cells than from changes in chemistry. Several quaternary Zn-Al-Mg-X alloys with improved corrosion stability in both open and crevice configurations were identified.

Keywords: Hot dip galvanized steel, alloy coatings, corrosion stability, corrosion testing, field exposure

INTRODUCTION

Zinc and zinc alloy coatings deposited by either electroplating or hot-dip galvanizing are crucial for corrosion protection of steel. In the last two decades, it turned out that Zn-Mg and Zn-Al-Mg alloys provide improved corrosion stability when compared to traditional zinc coatings[1–24]. There is a strong interest to investigate alternative alloying elements to Mg and Al and to evaluate their potential to enhance the corrosion protection provided by Zn, Zn-Mg, Zn-Al, and Zn-Al-Mg coatings.

The rate of zinc corrosion under atmospheric weathering conditions is usually controlled by the rate of oxygen reduction[25]. It is affected by the composition and structure of the oxide layer(s) covering the metal surface[26]. It was shown that oxygen adsorbs and reduces easily on surfaces covered with ZnO due to the rather good electrical conductivity of this oxide[27]. Modification of the oxide layer with alloying elements can reduce the electrical conductivity and improve coating corrosion properties. The aim of this study was to assess corrosion properties of a series of Zn-X, Zn-Mg-X, Zn-Al-X and Zn-Al-Mg-X cast alloys in order to select compositions for application as coatings for protection of steel car bodies.

MATERIALS

Three series of model cast alloys were prepared for this study. First, binary Zn-X and ternary Zn-Al-X and Zn-Mg-X alloys with target Al, Mg and X concentrations of 5, 6 and 2 wt.% were prepared. Zn-5Al is a eutectic composition produced commercially. Zn-6Mg with the composition close to the Mg_2Zn_{11} phase showed the best corrosion stability

from a number of Zn-Mg alloys containing 1–32 wt.% Mg[28]. As X, the following elements were selected: Ti, Ce, Zr, Mo, Cr, Si, Mn, B, Ga, In, Cu, Ni and Ca. Second, quaternary Zn-3Al-2Mg-X alloys were cast with the target concentration of X of 0.2, 0.6 and 2 wt.%. Third, materials selected in view of expected good performance in confined zones modelling hem flanges with Al content varying from 1 to 5 wt.% were prepared. A list of 69 cast materials is given in Table 1.

Table 1 Material denomination and composition

Denomination	Chemical composition [wt.%]				Denomination	Chemical composition [wt.%]			
	Zn	Al	Mg	X		Zn	Al	Mg	X
Zn	>99.9				Zn-6Al-2In	92.1	5.6		1.9
Zn-2Ti	97.3			1.7	Zn-6Al-2Cu	91.8	6.3		1.6
Zn-2Mm	96.8			1.9	Zn-8Al-2Ni	89.9	7.7		2.0
Zn-2Zr	97.5			1.8	Zn-6Al-1Ca	92.4	5.7		1.4
Zn-0.01Mo	99.5			0.01	Zn-0.01Si	>99.9			<0.01
Zn-0.6Cr	99.0			0.6	Zn-2Mg-0.6Cr	97.5		2.0	0.6
Zn-0.0003B	99.3			0.0003	Zn-3Al-0.6Cr	96.4	3.0		0.6
Zn-2Ga	97.5			1.8	Zn-3Al-2Mg	94.9	3.0	2.1	
Zn-2In	97.7			1.8	Zn-3Al-2Mg-0.2Cr	94.6	3.1	2.1	0.2
Zn-2Cu	98.0			1.7	Zn-3Al-2Mg-0.5Cr	94.8	3.1	2.0	0.5
Zn-2Ni	97.1			2.5	Zn-3Al-2Mg-0.2Zr	94.7	3.0	2.1	0.2
Zn-1Ca	98.0			1.5	Zn-3Al-2Mg-0.6Zr	94.3	3.1	2.0	0.6
Zn-2Mg	97.8		2.0		Zn-3Al-2Mg-2Zr	93.2	2.9	2.0	1.9
Zn-7Mg	93.0		6.8		Zn-3Al-2Mg-0.2Ti	94.6	3.1	2.0	0.2
Zn-2Al	97.8	2.1			Zn-3Al-2Mg-0.6Ti	94.3	3.1	2.0	0.6
Zn-3Al	96.6	3.1			Zn-3Al-2Mg-2Ti	92.6	3.1	2.1	2.1
Zn-5Al	94.7	5.2			Zn-3Al-3Mg-0.3Mm[1]	93.6	3.0	3.1	0.3
Zn-7Mg-1Ti	92.4		6.8	0.6	Zn-3Al-2Mg-0.6Mm[1]	94.1	3.1	2.1	0.6
Zn-7Mg-1Mm[1]	91.2		7.2	1.2	Zn-3Al-2Mg-0.01Mo	94.8	3.1	2.1	0.01
Zn-7Mg-2Zr	90.5		7.5	1.8	Zn-3Al-2Mg-0.2Mn	94.8	2.9	2.1	0.2
Zn-7Mg-0.01Mo	93.0		6.7	0.01	Zn-3Al-2Mg-0.6Mn	94.2	3.1	2.1	0.6
Zn-7Mg-0.5Cr	92.9		6.6	0.5	Zn-3Al-2Mg-2Mn	92.8	3.1	2.1	1.9
Zn-7Mg-0.004B	92.0		7.3	0.004	Zn-3Al-2Mg-2Si	93.1	3.0	2.0	1.9
Zn-10Mg-2Ga	87.3		10.4	2.0	Zn-2Al-3Mg	95.0	1.9	3.0	
Zn-6Mg-2In	92.1		6.1	1.8	Zn-1Al-2Mg	96.7	1.1	2.2	
Zn-7Mg-2Cu	90.9		6.8	2.1	Zn-1Al-2Mg-2Si	94.8	0.9	2.1	2.1
Zn-7Mg-2Ni	91.1		6.5	2.2	Zn-2Al-2Mg	95.9	2.0	2.1	
Zn-7Mg-1Ca	92.2		6.5	1.1	Zn-2Al-2Mg-2Si	93.9	1.9	2.1	2.1
Zn-8Al-2Ti	89.4	8.3		2.0	Zn-5Al-2Mg	93.0	4.8	2.2	
Zn-9Al-2Mm[1]	89.0	8.6		1.6	Zn-5Al-2Mg-2Si	90.9	5.0	2.0	2.2
Zn-7Al-1Zr	92.0	6.7		1.1	Zn-3Al-2Mg-0.2Si	94.9	2.9	1.9	0.2
Zn-8Al-0.01Mo	92.1	7.6		0.01	Zn-3Al-2Mg-0.6Si	94.5	2.9	1.9	0.6
Zn-6Al-0.4Cr	93.0	6.3		0.4	Zn-3Al-2Mg-0.2Ca	94.9	3.0	1.9	0.2
Zn-6Al-0.0003B	93.3	6.0		0.0003	Zn-3Al-2Mg-0.6Ca	94.3	3.1	2.1	0.6
Zn-6Al-2Ga	92.1	5.8		2.0	[1]Mm: Mischmetal, mixture of cerium and other lanthanides				

The model alloys were prepared by induction melting in a graphite crucible under argon protective atmosphere. Purity of raw materials was at least 99.5 wt.%. After introduction to a crucible, raw materials were heat up to 500–800 °C depending on the composition and kept at the temperature for up to 6 hours to dissolve and homogenize. Then, still under the protective atmosphere, the melt was poured into a brass mold. Cylindrical casts of 50 mm in diameter were cut to samples 2–4 mm thick. Before each experiment, they were polished down to 400 grit and their backsides masked with tape.

Microstructure of the alloys was studied after grinding, polishing and etching in 10% Nital solution by light and electron microscopy. Phase composition was analyzed by x-ray diffraction spectrometry (XRD) and energy dispersive x-ray spectroscopy (EDX). Chemical composition was measured by x-ray fluorescence (XRF).

As reference, hot dip panels of Zn-0.2Al (Z; coating weight 275 g/m²), Zn-5Al (ZA; 130 g/m²), Zn-55Al-1.6Si (AZ; 150 g/m²), Zn-1.5Al-1.5Mg (ZM; 190 g/m²) and Zn-11Al-3Mg-0.2Si (ZMM; 100 g/m²) were used. The panels were cut to 150×100 mm and backside and edges masked with tape.

EXPERIMENTAL PROCEDURE

ECC1. Renault ECC1 D17 2028 test is a cyclic accelerated corrosion test developed and used by the automotive industry. Four parallel samples of each composition were subjected to 42 daily cycles with total duration of six weeks. The cycle is performed at 35 °C and comprises wet (90 % relative humidity, RH) and dry (55 % RH) phases. Chloride solution with 1 wt.% NaCl at pH 4 is sprayed over the samples during 30 minutes once a day.

Field exposure. Selected materials were exposed at a marine test site "Base navale" in Brest, France. The site is characterized by high corrosivity of C5 and C3 for steel and zinc, respectively, due to elevated chloride deposition of 1 g/m² day or higher. The typical average yearly temperature is 13 °C, RH 85% and time of wetness 500 hours/month. Four replicates of 43 materials were exposed in November 2012 at 45° to horizontal facing south. Mass loss and corrosion depth were evaluated on two samples per composition after 10 and 24 months of exposure.

Mass loss after ECC1 and field exposure was measured after removal of corrosion products in saturated solution of glycine, NH_2CH_2COOH, in deionized water at laboratory temperature in an ultrasonic bath following the ISO 8407 standard. Although the procedure does not need to be optimal for all alloy compositions, obtained pickling curves were apparently correct. For AZ, chromic acid (100 g/L CrO_3, 10 g/L $AgNO_3$) solution was used.

Galvanic protection. A piece of an alloy material with soldered wire was attached to a piece of similarly prepared carbon steel with a 120-µm insulating polymer membrane separating them. The exposed area was from 50 to 125 mm² with identical alloy to steel ratio 1:1. A photograph and schematic drawing of a galvanic sample is seen in Figure 1.

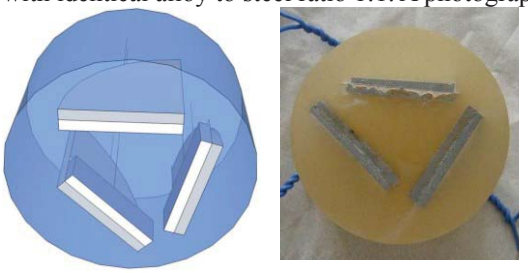

Figure 1 Schematic drawing (left) and photograph (right) of steel/alloy couples for galvanic protection experiments

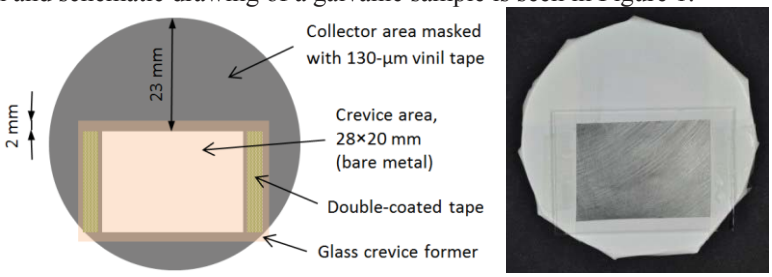

Figure 2 Schematic drawing (left) and photograph (right) of a crevice panel; diameter 50 mm

Open circuit and galvanic potential of the alloys and galvanic current flowing between carbon steel and the alloy were measured in artificial rain water (852 mg/L Na_2SO_4, 4.3 mg/L $MgCl_2$, 3.1 mg/L $CaCl_2$, 8.9 mg/L NaCl, 10.5 mg/L NH_4NO_3). The composition was adapted from a study of He et al.[29] to reflect properties of rain water in inland Europe. It was selected to model relatively low corrosive environments with limited content of chloride where alloyed materials might passivate. A galvanic couple was immersed in the solution for four weeks and electrochemical measurements repeatedly performed. To assess efficiency of the galvanic protection, steel parts were inspected visually and ranked based on the amount of formed corrosion products (red rust). A simple ranking system from 1 to 3 is described in Table 2.

Table 2 Ranking system for presence of red rust on steel in galvanic couples (alloy on top, steel in bottom)

Ranking	1	2	3
Description	No red rust	Slight red rusting	Heavy red rusting
Example		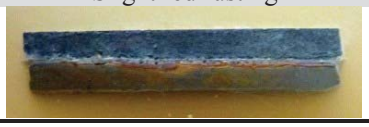	

Crevice panels. Because corrosion of hem flanges is critical for corrosion performance of car bodies, crevice samples of most cast materials were prepared. The sample design is seen in Figure 2. The confined zone was formed with a glass slide fixed by double-coated tape. The crevice opening had width of 130 µm. The width was verified using a calibrated metal foil. The crevice width (metal to glass) was 260 µm. The size of the exposed metal was 28×20 mm. The rest of the sample was masked with 130-µm vinyl tape. At least four parallel crevice samples for each material were exposed to ECC1 for six weeks. The crevices were filled with the NaCl solution used for sample spraying before the test.

It needs to be noted that due to several factors, the results are only comparative. First, because of small sample size, the setup is not conforming to any standard and the kinetics in in the crevice is thus specific. Second, typical duration of the test for hem flanges is twelve weeks, not six. Third, it was obviously impossible to assess the time to red rust appearance, which is usually the principal parameter to be followed.

RESULTS AND DISCUSSION

Test ECC1

The ECC1 test was carried out separately for three series of cast alloys. Each time, selected alloys and a set of reference panels were exposed. Although the exposure conditions were apparently identical, there were differences in obtained mass losses in parallel tests. For example, mass loss of cast Zn with purity >99.9 wt.% was 86±8, 85±6 and 67±2 g/m². Thus, instead of absolute mass loss values, a relative drop in mass loss compared to mass loss of cast zinc exposed in the same test was used as a measure of the effect of alloying. The drop D expressed in % is defined by Eq. (1), where Δm stands for mass loss in g/m². Results are shown in Figure 3. Only selected binary and ternary materials are displayed in sake of clarity.

$$D = \frac{\Delta m_{Zn} - \Delta m_{alloy}}{\Delta m_{Zn}} \qquad (1)$$

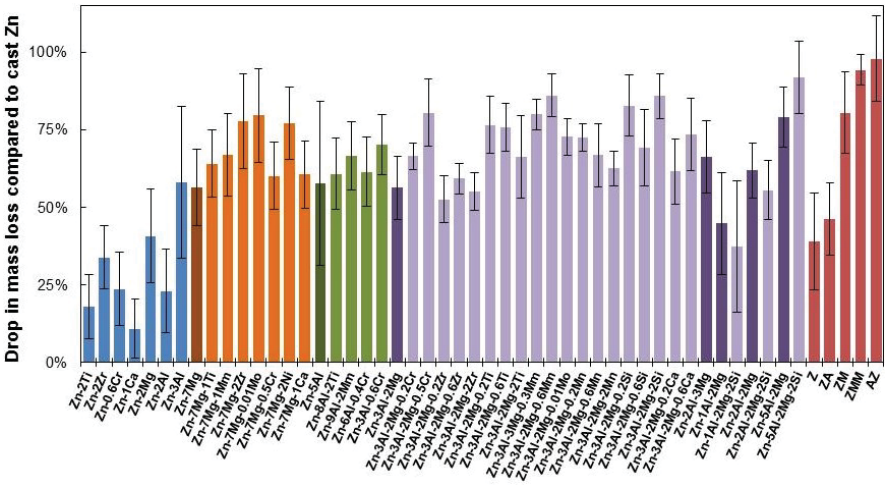

Figure 3 Drop in mass loss of selected model alloys and reference materials compared to cast zinc after 6 weeks in ECC1 test

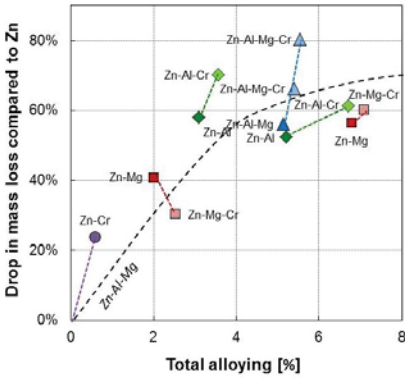

Figure 4 Combined effect of alloying with Al and Mg (black curve) and Cr (color curves) on drop in mass loss compared to Zn for alloys exposed to ECC1

Most reference panels showed about 2-fold lower mass loss than cast alloys with corresponding composition. This may indicate the importance of the material microstructure, which is clearly different for coatings and for cast alloys. It also suggests that the performance of the alloyed materials might further improve when applied as coatings.

In binary alloys, Mg and Al had the strongest inhibiting effect. Ti, Zr, Cr and Ca reduced mass loss of zinc by 11–34%. In ternary alloys, none of the third elements provided any substantial improvement in corrosion stability. Quaternary Zn-3Al-2Mg-X alloys outperformed the ternary ones providing 70% improvement to zinc in average.

The chart in Figure 4 shows the effect of Al, Mg and Cr. Al and Mg improved the zinc corrosion stability in a similar extent and their effect was additive. This was reported earlier in conditions of another accelerated corrosion test[12]. An important improvement in mass loss due to Al and Mg was seen up to about 4 wt.% of the total alloying. The effect of *chromium* was low in ternary alloys with Mg. A stronger improvement was observed when combined with Al. Five-fold improvement in mass loss was observed for Zn-3Al-2Mg-0.5Cr. *Silicon* provided very high inhibition efficiency in Zn-3Al-2Mg-2Si with seven-fold lower mass loss compared to Zn. It also improved corrosion stability of Zn-5Al-2Mg . Zn-5Al-2Mg-2Si was more than 10-fold less corroded than cast zinc. Zn-1Al-2Mg-2Si and Zn-2Al-2Mg-2Si were more corroded than the base alloys. Except for Zn-2Mm, *mischmetal (cerium)* improved the stability of all alloys. It was particularly efficient in Zn-3Al-2Mg-Mm. The effect was strong already at 0.3 wt.% Mm but further increased for Zn-3Al-2Mg-0.6Mm, which provided seven-fold improvement to Zn. *Titanium* was inhibiting corrosion in Zn-2Ti but the effect in ternary alloys was low. In quaternary alloys, Ti seems to be most efficient at lower additions with the best stability demonstrated by Zn-3Al-2Mg-0.2Ti. Considering very low solubility of *molybdenum* in zinc and the alloys, it showed surprisingly strong effect when combined with Mg or with Al and Mg. The effect of Mo addition to Zn and Zn-Al was negligible. Most successful was Zn-7Mg-0.01Mo with 80% improvement to Zn. The effect of *manganese* seems to be the most positive at lower concentrations. Zn-3Al-2Mg-0.2Mn outperformed the materials with 0.6 and 2 wt. % Mn. Alloying with other elements led to small improvements.

In summary, no binary or ternary alloys except of Zn-Mg, Zn-Al and Zn-Al-Mg showed particularly good results in the ECC1 test. Several quaternary Zn-Al-Mg-X alloys gave low mass loss.

Galvanic protection

To provide galvanic protection to steel on cut edges and in defects, open corrosion potential, E_{OC}, of a metallic coating must be sufficiently negative to that of steel. E_{OC} of the model alloys measured after 30 minutes of stabilization in artificial rain water was in a range from –1120 to –800 mV/SCE, i.e. safely negative to carbon steel at about –600 mV/SCE. Since corrosion products can passivate the surface, galvanically coupled alloy/steel assemblies were kept in the environment for four weeks and the E_{OC} re-measured 10 minutes after disconnection. In average, it moved by only 40 mV to more positive values. Except for Zn-7Mg-0.01Mo with E_{OC} increasing to –490 mV/SCE and becoming thus cathodic to steel, the alloys provided good galvanic protection to steel even in the low-aggressive electrolyte.

Galvanic current flowing between steel and alloy electrodes was measured by zero resistance ammetry (ZRA) 30 minutes after immersion. Most alloyed materials provided higher galvanic current compared to Zn, i.e. better ability to protect steel. This is particularly true for Zn-Al-Mg(-X) alloys with 2-fold higher galvanic current in average. In four weeks of exposure, it dropped by an order of magnitude. Magnesium addition tended to lower the galvanic current, whereas aluminum increased it. The alloying with X had a limited effect.

Visual appearance of steel electrodes after four weeks of exposure to the artificial rain water under galvanic protection was ranked using the system described in Table 2. Results are plotted in Figure 5. Only four alloys protected steel from red rust formation to a lesser extent than Zn: Zn-2Ti, Zn-7Mg-1Ti, Zn-7Mg-0.01Mo and Zn-6Al-2Cu. With a few exceptions, Zn-Al-Mg(-X) materials were more protective than Zn. The visual ranking principally agrees to the galvanic current measurements after four weeks of stabilization. Zn-Al-X alloys were more protective than Zn-Mg-X alloys and the binary Zn-X alloys ranked in between. Superior performance showed Zn-Al-Mg-X materials.

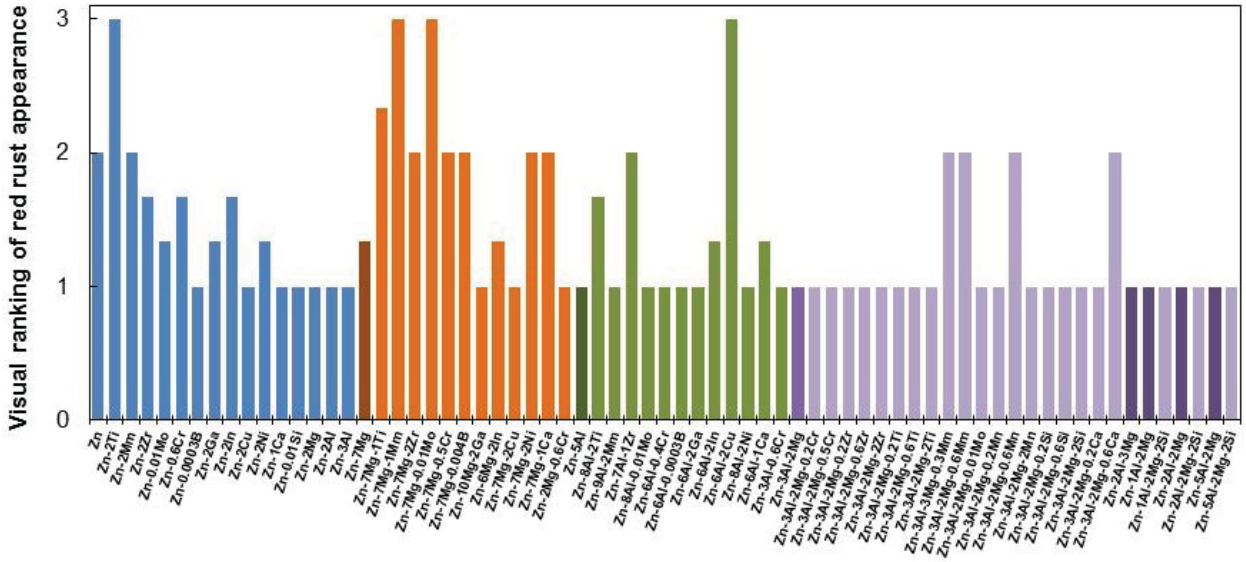

Figure 5 Visual ranking of red rust appearance on steel electrodes after four weeks of galvanic coupling in artificial rain water; for the ranking system, see Table 2

Field exposures

Mass loss of two replicate samples was measured after 10 months. Two more samples were assessed after 24 months of exposure. The latter data for all materials and both data sets for Zn-Al-Mg-X alloys are presented in Figure 6.

Large difference in mass loss was observed between cast Zn and reference line Z panels. When compared to rolled zinc of 99.9% purity used for site calibration, Z gave similar mass loss. Thus, an origin of this discrepancy cannot be the small amount of aluminum present in Z. No major impurities were found in the structure of the cast Zn samples by EDX.

When the reference panels are considered, mass loss dropped by 40 % due to alloying with 2 wt.% of Al and Mg compared to Z. ZA outperformed ZM in both periods. It gave 3-fold lower mass loss than Z. The best results showed AZ with three- and four-times lower mass loss to Z after 10 and 24 months of exposure, respectively. The difference between Z and the alloyed coatings tended to increase with exposure time. It should be noted that a single panel of each reference material was available after 24 months of exposure. The relative error of measurement is expected to be similar as after 10 months when three replicates were assessed, i.e. about 7 %.

Binary Zn-X alloys with Zr and Cr were less corroded than Zn. Ti, Mm, Ca and Si showed only a minor inhibiting effect. Mass loss of Zn-7Mg was only slightly lower than for Zn. Zn-5Al was the least corroded of all binary alloys. The

stronger inhibiting effect of aluminum in the marine climate compared to conditions of the accelerated corrosion test, compare Figure 3 and Figure 6, is in line with earlier results[24]. All ternary Zn-Mg-X alloys were somewhat less corroded than Zn-7Mg but the difference was not large. No Zn-Al-X ternary alloy outperformed Zn-5Al.

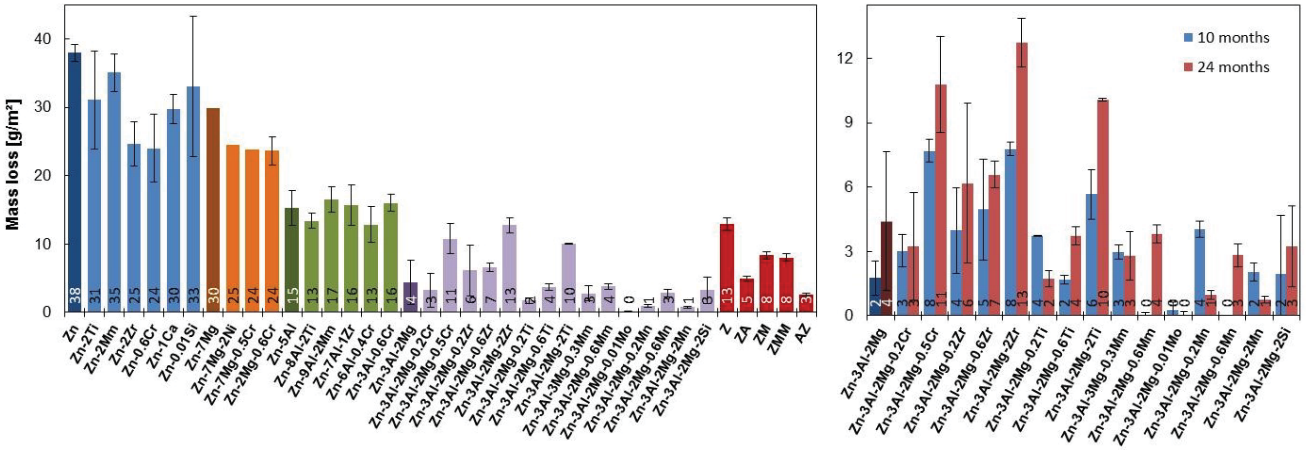

Figure 6 Mass loss of model alloys and reference materials after 24 months of field exposure; error for reference materials is estimated based on 10-month data (left); data after 10 and 24 months for Zn-Al-Mg-X alloys (right)

Zn-3Al-2Mg and corresponding quaternary alloys showed the best corrosion stability. The lowest mass loss was measured for Zn-3Al-2Mg-0.01Mo and alloys containing Mn. Promising are also results for Zn-3Al-2Mg-0.2Cr, Zn-3Al-2Mg-0.2Ti, Zn-3Al-2Mg-0.6Ti, Zn-3Al-2Mg-0.3Mm, Zn-3Al-2Mg-0.6Mm and Zn-3Al-2Mg-2Si.

The results need to be considered in view of the experimental error of the pickling operation (removal of corrosion products), which can reach 2–4 g/m² for the small samples of cast alloys. Since most of the Zn-3Al-2Mg-X materials were very stable, any ranking is only indicative. Anyway, the data show on a strong synergy between Al and Mg in marine exposure conditions. Zn-7Mg and Zn-5Al were significantly more corroded than Zn-3Al-2Mg with similar total content of alloying elements.

Corrosion in confined zones

The crevice panels were exposed to ECC1 in three sets. Several alloys have been exposed repeatedly, e.g. Zn, each time with four replicates. Variation in mass loss of crevice panels between the tests was similar or even lower than between parallel samples in an identical test with mass loss of 178±24, 225±5 and 216±73 g/m² for Zn.

Mass loss in crevice and open configurations under identical testing conditions for selected alloys is given in Figure 7. The scatter in the crevice configuration was larger than on open surfaces. It is observed regularly for this type of setup due to the importance of transport from and to the confined zone, which can be easily altered by e.g. blocking of the crevice opening with corrosion products or small variations in sample geometry.

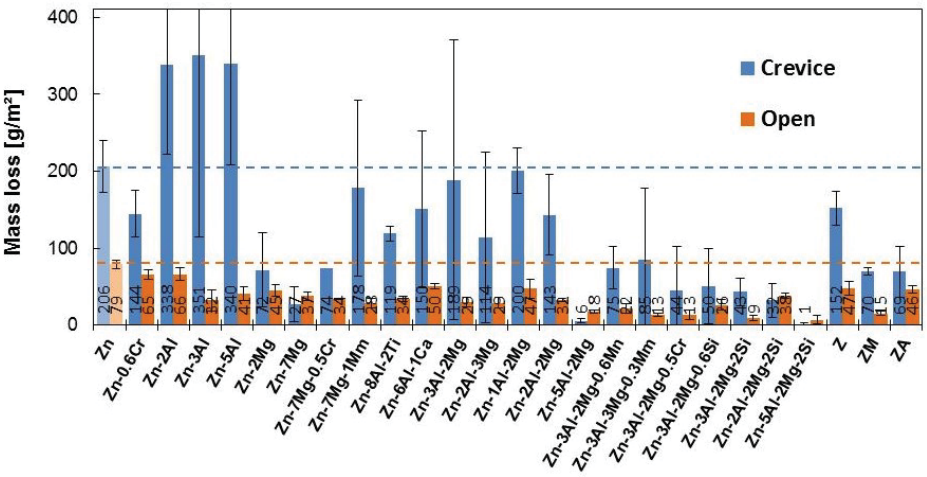

Figure 7 Mass loss in crevice and open configuration after 6 weeks in ECC1 test

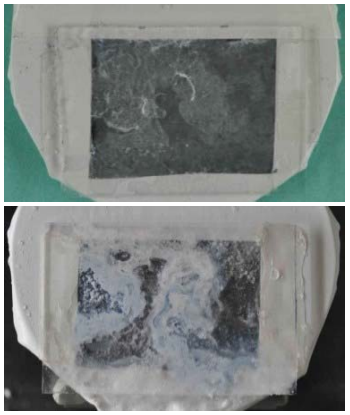

Figure 8 Photographs of Zn-2Mg (top) and Zn-5Al (bottom)

In next paragraphs, the results are discussed for separate groups of alloys in terms of absolute mass loss in crevices and ratios of mass loss in the crevice vs. open configuration.

For cast Zn and line Z, the mass loss increased by a factor of 2–3 in the confined zone. It is a rather typical value although it depends on exact crevice geometry and accelerated test[12]. It shows that the setup was principally correct.

A dramatic increase in mass loss in the confined zone was measured for all binary alloys containing aluminum (Figure 8, bottom). It was 5- to 11-times higher than on the open surface. Inhibition due to Al alloying observed on open surfaces fully disappeared in the confine zone. Interestingly, reference ZA performed 2-times better than Z in the crevice.

Alloys with magnesium provided the best performance of all binary alloys in the confined zone (Figure 8, top). They gave similar mass loss in both configurations showing on potentially exceptional resistance to perforation corrosion.

The detrimental effect of aluminum and strong inhibition with magnesium may explain results of earlier studies showing very good performance of Zn-Mg coatings prepared by physical vapor deposition[8] and rather non-impressive results for Zn-Al-Mg materials produced by hot dipping[12] in model crevices. It is possible that the performance of the latter group of materials is negatively affected by the presence of aluminum. However, relatively good results for commercial ZA suggest that the unfavorable role of aluminum does not need to be due to its direct chemical role in corrosion processes but rather due to changing microstructure. ZA has a two-phase lamellar eutectic structure with no primary zinc dendrites at the air/coating interface[30]. The model Zn-Al alloys contained both primary zinc dendrites and the eutectics, which is probably disadvantageous in view of formation of micro-galvanic cells and strong pH separation.

On several Zn-Al-Mg alloys, it was tested whether the negative effect of aluminum could be compensated by the Mg alloying. Results seem to suggest that whatever the Al to Mg mass ratio in a range from 1:2 to 3:2, the Zn-Al-Mg did not provide any improvement in crevices, i.e. behaved closer to Zn and Zn-Al than to Zn-Mg. The ratio of mass loss in crevice vs. open varied from 4 to 8 for Zn-Al-Mg. Results for commercial ZM were basically in agreement. Although it was 2-times less corroded in the crevice than Z, the mass loss increased close to 5-times compared to the open surface. Good performance in the model crevice gave only Zn-5Al-2Mg with negligible mass loss.

To verify whether any alternative alloying element would have as strong inhibiting effect in the crevice configuration as magnesium, a series of Zn-X materials were tested. With exception of chromium, none of X provided any improvement in crevices. The crevice vs. open mass loss ratio was in between 2 and 3 for all binary alloys.

Then, it was examined if any element can further improve the performance of Zn-Mg or reduce the negative effect of Al. Both Zn-7Mg-0.5Cr and Zn-7Mg-1Mm were more corroded in the crevice than Zn-7Mg. Most Zn-Al-X alloys were corroded similar to Zn-5Al. Zn-8Al-2Ti and possibly Zn-6Al-1Ca performed better in crevices than Zn-Al alloys with the crevice to open mass loss ratio of 3.5 and 3. However, the inhibition effect was weak compared to Mg.

Finally, it was investigated if any element can improve the corrosion stability of Zn-Al-Mg in crevices. Due to very high scatter for eight samples of Zn-3Al-2Mg in two tests, the data are non-conclusive. It seems that most elements efficient in the open configuration were little inhibitive in crevices. Promising results were obtained for Zn-3Al-2Mg alloyed with 0.6% Mn, 0.3% Mm and 0.5% Cr. The best performance showed repeatedly materials containing silicon. In particular, Zn-5Al-2Mg-2Si, Zn-2Al-2Mg-2Si, Zn-3Al-2Mg-2Si and Zn-3Al-2Mg-0.6Si gave low mass loss in the crevice configuration. Visual appearance of these samples was also superior with a low amount of corrosion products.

Basic comparison of microstructures of more and less stable alloys in confined zones suggests that those with a finer phase distribution tended to perform better. This can be shown for Si alloyed Zn-Al-Mg, see Figure 9. With a finer microstructure, lower acceleration of corrosion by local galvanic microcells can be expected.

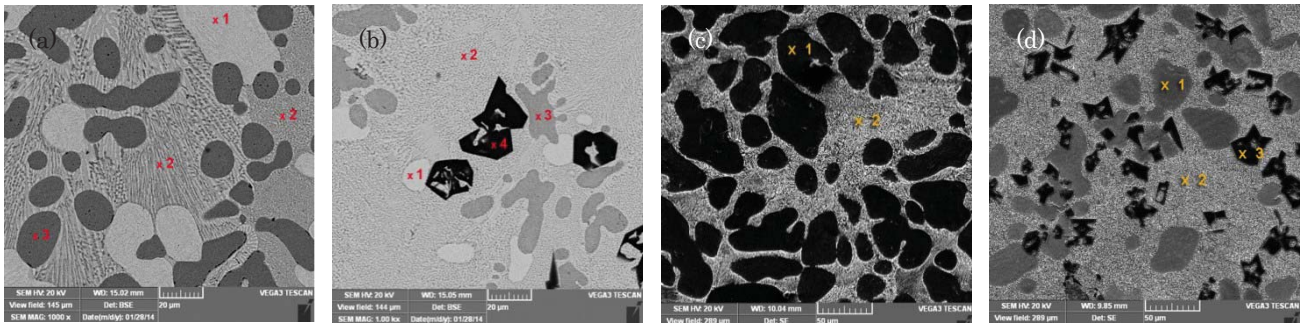

Figure 9 Microstructure of Zn-5Al-2Mg (a), Zn-5Al-2Mg-2Si (b), Zn-3Al-2Mg (c) and Zn-3Al-2Mg-2Si (d); 1: η-phase (Zn-rich), 2: Eutectics η + α + Mg_2Zn_{11}; 3: α-phase (Al rich); 4: Si particles

The effect of alloying elements was thus different in open and crevice configurations. There were elements inhibiting corrosion in both configurations (in particular Mg, but – in a decreasing order – also Si, Cr, Mn and Ti) as well as those efficient only on open surfaces (Al) or only in crevices (possibly Ca).

MATERIAL RANKING

Improvements in corrosion stability provided by alloying compared to non-alloyed cast Zn in the above-discussed laboratory tests as well as in several others not described in this paper were weighted based on the expected importance of each test for material performance in service conditions. Similarly, outdoor performance relative to cast Zn was established by weighting the data on mass loss after 10 and 24 months and corrosion depth after 10 months. Improvement factors in the crevice configuration were also obtained.

The best materials in open and crevice configurations in accelerated tests and in the open configuration at a marine test site are listed in Table 3. Several ternary Zn-Al-Mg alloys were highly corrosion resistant with the best results for Zn-5Al-2Mg. Only one more ternary alloy is in the Top-10 lists, Zn-7Mg-0.5Cr with a good stability in the crevice configuration. From binary alloys, only Zn-2Mg and Zn-7Mg with superior stability in model crevices are included. It is well apparent that the best performance provided quaternary Zn-Al-Mg-X alloys. Based on all three criteria, Zn-3Al-2Mg-2Si and Zn-3Al-2Mg-0.5Cr can be considered most corrosion resistant. They gave an improvement to Zn of 79–81% (4-fold) and 72–79% (3-fold), respectively. Zn-5Al-2Mg-2Si was not exposed outdoors but very successful in accelerated tests with the improvement from 85 to 99%.

Table 3 Top-10 best performing materials

Open, laboratory		Open, field		Crevice, laboratory	
Material	Impr.	Material	Impr.	Material	Impr.
Zn-5Al-2Mg-2Si	85%	Zn-3Al-2Mg-0.6Mn	91%	Zn-5Al-2Mg-2Si	99%
Zn-3Al-2Mg-2Si	80%	Zn-3Al-2Mg-2Mn	91%	Zn-5Al-2Mg	97%
Zn-3Al-2Mg-0.5Cr	79%	Zn-3Al-2Mg-0.01Mo	91%	Zn-7Mg	87%
Zn-3Al-2Mg-0.2Si	79%	Zn-3Al-2Mg-0.2Ti	91%	Zn-2Al-2Mg-2Si	84%
Zn-5Al-2Mg	76%	Zn-3Al-2Mg-0.6Mm	91%	Zn-3Al-2Mg-2Si	79%
Zn-3Al-2Mg-0.2Mn	74%	Zn-3Al-3Mg-0.3Mm	90%	Zn-3Al-2Mg-0.5Cr	78%
Zn-3Al-2Mg-0.01Mo	74%	Zn-3Al-2Mg-0.2Mn	87%	Zn-3Al-2Mg-0.6Si	76%
Zn-3Al-2Mg-0.2Ti	74%	Zn-3Al-2Mg-0.2Cr	87%	Zn-2Mg	65%
Zn-3Al-2Mg-0.6Si	71%	Zn-3Al-2Mg-0.6Ti	83%	Zn-7Mg-0.5Cr	64%
Zn-2Al-3Mg	71%	Zn-3Al-2Mg	83%	Zn-3Al-2Mg-0.6Mn	64%

Impr.: An improvement factor to cast Zn

Besides magnesium, strong inhibiting effect on corrosion in both open and crevice geometries had only silicon. In this view, silicon is the most attractive alloying element of Zn-Al-Mg.

It was shown that small additions of Si, Cr, Ce (Mm), Mn, Mo and Ti can increase corrosion stability of Zn-Al-Mg alloys, mostly at lower concentrations up to 0.6 wt.%. It only needs to be proved in further tests if the improvement is strong enough to be technically interesting in view of increased production complexity and costs.

The approach used in this study, i.e. to work with a large number of model cast alloys, led to identification of compositions with interesting anti-corrosion properties. However, there are limitations of this approach connected to different microstructures of cast alloys and coatings. Obviously, tests of coated steel samples have to follow.

CONCLUSIONS

Corrosion stability of 69 model alloys has been assessed in accelerated tests and in marine atmosphere. On open surfaces, the potential of Mg and Al to inhibit zinc corrosion was repeatedly demonstrated. It was beneficial to combine both elements, especially in outdoor exposure conditions. The corrosion stability of Zn-Al-Mg can be further improved by addition of a fourth element. Quaternary Zn-Al-Mg-X alloys provided strong improvement in corrosion stability compared to non-alloyed zinc. In general, they outperformed binary Zn-X and ternary Zn-Al-X and Zn-Mg-X materials.

Except for Zn-7Mg-0.01Mo, the alloys provided good galvanic protection to steel in defects. Zn-Al-X alloys were more protective than Zn-Mg-X. Superior galvanic protection potential was revealed for Zn-Al-Mg-X.

Strong inhibition with Mg and detrimental effect of Al in confined zones simulating hem flanges was found. It is expected that the detrimental effect of aluminum was more because of coarser microstructures leading to formation of micro-galvanic cells than due to changes in chemistry of the electrolytes. Alloying of Zn-Al-Mg with silicon inhibited corrosion in confined zones. It was probably due to finer phase distribution.

Materials with good anti-corrosion properties under multiple exposure conditions with application potential for use in car bodies were identified. Zn-3Al-2Mg-2Si, Zn-3Al-2Mg-0.5Cr, Zn-5Al-2Mg-2Si, Zn-3Al-2Mg-0.6Si, Zn-3Al-2Mg-0.6Mn, Zn-3Al-2Mg-2Mn and Zn-3Al-2Mg-0.01Mo are considered most promising.

ACKNOWLEDGEMENTS

All members of the Galvanized Autobody Partnership program are thanked for their valuable inputs. We wish to thank Jan Šerák of Institute of Chemical Technology, Prague for the preparation and characterization of the alloys. Cecile Hall, Anne Le Gac and Vanessa Le Vern of Institut de la Corrosion are thanked for technical assistance with the corrosion experiments.

REFERENCES

1. M. Morishita, K. Koyama, Y. Mori, Materials Transactions JIM 38 (1997) 719–723.
2. K. Nishimura, H. Shindo, K. Kato, Y. Morimoto, Microstructure and corrosion behaviour of Zn-Mg-Al hot dip galvanized steel sheet, Proc. of Galvatech '98, Chiba, Japan (1998), pp. 437–442.
3. T. Tsujimura, A. Komatsu, A. Andoh, Influence of Mg content in coating layer and coating structure on corrosion resistance of hot-dip Zn-Al-Mg alloy coated steel sheet, Proc. of Galvatech '01, Brussels, Belgium (2001), pp. 145–152.
4. R. Hausbrand, M. Stratmann, M. Rohwerder, Delamination resistant zinc alloys: Simple concept and results on the system zinc-magnesium, Steel Research International 74 (2003) 453–458.
5. T. Koll, K. Ullrich, J. Faderl, J. Hagler, A. Spalek: Properties and potential applications of ZnMg-alloy-coatings on steel sheet by PVD, Proc. of Galvatech '04, Chicago, IL, United States, p. 803–812, April 4–7, 2004.
6. M. Vlot, R. Bleeker, T. Maalman, E. van Perlstein: MagiZincTM: A new generation of hot-dip galvanised products, Proc. of Galvanized Steel Sheet Forum, ILZRO and IZA, Dusseldorf, Germany, 2006.
7. N. C. Hosking, M. A. Strom, P. H. Shipway, C. D. Rudd, Corrosion Science 49 (2007) 3669–3695.
8. N. C. Hosking, M. A. Strom, P. H. Shipway, C. D. Rudd: Next generation galvanized steel for the automotive industry, presented at EUROCORR, Freiburg im Breisgau, Germany, September 9–13, 2007.
9. R. Hausbrand, M. Stratmann, M. Rohwerder, Corrosion Science 51 (2009) 2107–2114.
10. S. Schürz, M. Fleischanderl, G.H. Luckeneder, K. Preis, T. Haunschmied, G. Mori, A.C. Kneissl, Corrosion Science 51 (2009) 2355–2363.
11. P. Volovitch, C. Allely, K. Ogle, Corrosion Science 51 (2009) 1251–1262.
12. T. Prosek, N. Larché, M. Vlot, F. Goodwin, D. Thierry D, Materials and Corrosion 60 (2010) 412–420.
13. S. Schürz, G. H. Luckeneder, M. Fleiscanderl, P. Mack, H. Gsaller, A.C. Kneissl, G. Mori, Corrosion Science 52 (2010) 3271–3279.
14. P. Volovitch, T. N. Vu, C. Allely, A. Abdel Aal, K. Ogle, Corrosion Science 53 (2011) 2437–2445.
15. O. Zywitzki, T. Modes, B. Scheffel, C. Metzner, Practical Metallography 49 (2012) 210–220.
16. N. LeBozec, D. Thierry, M. Rohwerder, D. Persson, G. Luckeneder, L. Luxem, Corrosion Science 74 (2013) 379–386.
17. D. Persson, D. Thierry, N. LeBozec, T. Prosek, Corrosion Science 72 (2013) 54–63.
18. J. Duchoslav, M. Arndt, R. Steinberger, T. Keppert, G. Luckeneder, K.H. Stellnberger, J. Hagler, C.K. Riener, G. Angeli, D. Stifter, Corrosion Science 83 (2014) 327–334.
19. T. Prosek, D. Persson, J. Stoulil, D. Thierry, Corrosion Science 86 (2014) 231–238.
20. T. Lostak, A. Maljusch, B. Klink, S. Krebs, M. Kimpel, J. Flock, S. Schulz, W. Schuhmann, Electrochimica Acta 137 (2014) 65–74.
21. J. Duchoslav, R. Steinberger, M. Arndt, T. Keppert, G. Luckeneder, K.H. Stellnberger, J. Hagler, G. Angeli, C.K. Riener, D. Stifter, Corrosion Science 91 (2015) 311–320.
22. M. Salgueiro Azevedo, C. Allély, K. Ogle, P. Volovitch, Corrosion Science 90 (2015) 472–481.
23. M. Salgueiro Azevedo, C. Allély, K. Ogle, P. Volovitch, Corrosion Science 90 (2015) 482–490.
24. T. Prosek, A. Nazarov, A. Le Gac, D. Thierry, Progress in Organic Coatings, accepted for publication.
25. I. L. Rosenfeld: Atmospheric Corrosion of Metals. Some questions of theory, Proc. of 1st International Congress on Metallic Corrosion, London, p. 243–253, April 1961.
26. C. Deslouis et al., Journal of Electroanalytical Chemistry 181 (1984) 119–136.
27. V. E. Henrich, P. A. Cox: The surface science of metal oxides, Cambridge University Press, 2000.
28. T. Prosek, A. Nazarov, U. Bexell, D. Thierry, J. Serak, Corrosion Science 50 (2008) 2216–2231.
29. W. He, I. Odnevall Wallinder, C. Leygraf, Water, Air and Soil Pollution 1 (2001) 67–82.
30. J. Elvins, J. A. Spittle, J. H. Sullivan, D. A. Worsley, Corrosion Science 50 (2008) 1650–1658.